Ideal Hydrodynamics for Bulk and Multistrange Hadrons in $\sqrt{s_{NN}}$=200 AGeV Au-Au Collisions

Min He,[1] Rainer J. Fries,[1, 2] and Ralf Rapp[1]

[1]*Cyclotron Institute and Department of Physics & Astronomy, Texas A&M University, College Station, TX 77843-3366, USA*

[2]*RIKEN/BNL Research Center, Brookhaven National Laboratory, Upton, NY 11973, USA*

(Dated: June 15, 2018)

We revisit the use of ideal hydrodynamics to describe bulk- and multistrange-hadron observables in nuclear collisions at the Relativistic Heavy Ion Collider. Toward this end we augment the 2+1-dimensional code "AZHYDRO" by employing (a) an equation of state based on recent lattice-QCD computations matched to a hadron-resonance gas with chemical decoupling at $T_{\rm ch} \simeq$160 MeV, (b) a compact initial density profile, (c) an initial-flow field including azimuthal anisotropies, and (d) a sequential kinetic decoupling of bulk (π, K, p) and multistrange (ϕ, Ξ, Ω) hadrons at $T \simeq 110$ MeV and 160 MeV, respectively. We find that this scheme allows for a consistent description of the observed chemistry, transverse-momentum spectra and elliptic flow of light and strange hadrons.

PACS numbers: 25.75.Dw, 12.38.Mh, 25.75.Nq

Keywords: Relativistic Hydrodynamics, Relativistic Heavy-Ion Collisions, Quark-Gluon Plasma

I. INTRODUCTION

Experiments at the Relativistic Heavy Ion Collider (RHIC) and the Large Hadron Collider (LHC) [1, 2] suggest that a quark gluon plasma (QGP) is created in ultra-relativistic heavy-ion collisions (URHICs) which is strongly coupled and behaves like a near-perfect liquid [3, 4]. In particular, the use of ideal relativistic hydrodynamics enabled a good description of several bulk hadron-observables encompassing more than 90% of the produced particles [5–14]. A rapid thermalization of the medium, leading to collective phenomena including elliptic flow, could be established and are key to our understanding of the macroscopic properties of the fireball. The success of ideal hydrodynamics and the conclusion that dissipative effects appear to be small has more recently led to efforts to quantify these by employing second-order viscous hydrodynamics [15–23]. This goal clearly requires a good control over any remaining uncertainties within the hydrodynamic framework, e.g., the equation of state (EoS), initial conditions and implementations of the freezeout scenario and/or final-state transport.

Some of these aspects and their interplay, common to both ideal and viscous hydrodynamics, are not well understood to date. For example, the elliptic flow, v_2, calculated in ideal hydrodynamics seemed to favor an EoS with a strong first order phase transition [24], contradicting the finite-T cross-over transition now firmly established in lattice quantum chromodynamics (QCD) [25, 26]. On the other hand, the recent progress in solving the so-called Hanbury Brown-Twiss (HBT) puzzle required several effects to increase the transverse expansion, including viscosities, initial flow and a hard EoS without phase transition [27]. The development of initial flow, prior to the thermalization time assumed in hydrodynamics, can be expected on rather general grounds [28, 29], but has only been studied in few works to date [8, 27, 30–32]. The initial density profile and initial fluctuations are not yet well constrained from first principles, with both Glauber- and Color-Glass Condensate (CGC)-based approaches currently being investigated [33, 34]. If dissipative effects become large, a transition to a transport treatment of the bulk is in order, which has been studied by coupling hadronic cascades to hydrodynamic evolutions of the QGP [10, 19, 33, 35]. However, it is quite possible that the viscosity in the hadronic phase remains small for a significant range of temperatures below T_c, especially if partial chemical equilibrium is implemented. The latter becomes problematic in cascade models if the inverse of reactions with multi-particle final states need to be accounted for, as, e.g., for baryon-antibaryon annihilation into mesons [36, 37]. To date, sequential chemical and thermal freezeouts in URHICs are experimentally well established, signified by statistical-model fits to hadron abundances [38–40] on the one hand (yielding $T_{\rm ch} \approx 160$ MeV), and empirical blast-wave fits to transverse-momentum (p_T) spectra of bulk hadrons (π, K, p) [38] on the other hand (yielding $T_{\rm fo} \approx 100$ MeV). In the hadronic EoS figuring into hydrodynamics the number conservation of stable hadrons (π, K, p, $\bar{p}$, η, etc.) between $T_{\rm ch}$ and $T_{\rm fo}$ can be enforced by introducing pertinent chemical potentials [41]. This has been implemented into ideal hydrodynamic models [7, 8, 42, 43]. It was found that bulk-hadron p_T spectra can be reproduced well at $T_{\rm fo}$, but the previous agreement with the observed elliptic flow, $v_2(p_T)$, deteriorates [8, 43, 44], i.e., it is overpredicted. In viscous hydrodynamics, a systematic investigation of the effects of chemical freezeout on bulk observables are still in their beginnings [21, 45, 46].

The spectra and v_2 of multistrange particles have received relatively little attention in hydrodynamic calculations thus far. The ϕ, Ξ and Ω have no well established resonances with bulk hadrons, and elastic t-channel exchange processes are suppressed by the Okubo-Zweig-Iizuka (OZI) rule. Therefore, multistrange hadrons are not expected to undergo significant rescattering in the hadronic phase and should decouple from the system early [47, 48]. This is supported by experimental data from RHIC [1, 49, 50]. Compared to bulk hadrons multistrange particles thus reflect more directly the collective dynamics of the partonic stage of the fireball and can provide a significant but often neglected constraint on hydrodynamic evolution models. For example, in the 2+1-dimensional hydro-simulations of Ref. [5], Ω^- freezeout has to be carried well into the hadronic phase to be compatible with the experimental p_T spectra.

In this work we will revisit to what extent *ideal* hydrodynamics is capable of providing a realistic description of the bulk evolution of the medium in Au-Au collisions at RHIC. With "realistic" we mean, on the one hand, a consistent description of light- and strange-hadron observables encompassing their abundances, p_T-spectra and $v_2(p_T)$ at midrapidity for semi-/central collisions. On the other hand, we also refer to inputs to, and assumptions in, the hydrodynamic treatment which are within the uncertainties described above. This includes (i) a state-of-the-art equation of state adopted from lattice QCD in the QGP phase, matched to a hadron resonance gas with hadrochemical freezeout; (ii) a sequential freezeout of bulk-hadron chemistry and kinetics, as well as simultaneous kinetic and chemical freezeout of multistrange hadrons (at the universal chemical freezeout); (iii) a compact initial density profile with relatively large gradients and "reasonable" initial radial and elliptic flow. We will also elaborate on arguments why the viscosity in the hadronic phase of URHICs could be rather small. We will, however, neglect the role of initial-state fluctuations, which are presumably the main source of higher flow harmonics, but do not seem to affect $v_{0,2}$ much [20].

Our computations build on the existing and readily available ideal hydrodynamic code package AZHYDRO developed by Kolb and Heinz [5]. One of our goals in performing a tune of AZHYDRO is to provide an easily accessible yet realistic background medium for quantitative applications to electromagnetic and heavy-flavor probes. In particular, we do not imply to supersede emerging viscous hydrodynamic calculations, which, once fully developed, are expected to become the tool of choice.

Our article is organized as follows. In Sec. II we briefly recall the basic features of the 2+1 dimensional hydrocode AZHYDRO and then focus on its amendments as applied in the present work. In Sec. III, we analyze the qualitative impact of our amendments on the evolution of the bulk medium, i.e., its radial and elliptic flow, and potential ramifications for hadron spectra, especially freezeout properties. In Sec. IV, we conduct quantitative fits to bulk- and multistrange-hadron observables, encompassing multiplicities, p_T spectra and elliptic flow. We summarize and conclude in Sec. V.

II. AZHYDRO AND ITS AMENDMENTS

The starting point for ideal hydrodynamics (IH) are the equations for the conservation of energy and momentum,

$$\partial_\mu T^{\mu\nu} = 0 \ , \tag{1}$$

formulated in terms of the energy-momentum tensor, $T^{\mu\nu}$. As usual, the latter is given by the energy density, e, and pressure, p, in the local rest frame assuming kinetic equilibrium, together with a flow field $\mathbf{v}$ describing the collective motion of the fluid cells. Other conserved currents (e.g., for baryon number), can be introduced as appropriate, see, e.g., Refs. [5, 9] for reviews. The system has to be closed by specifying an equation of state $p(e)$, initialized at a thermalization time τ_0 (typically with an initial entropy density and flow field) and frozen out in the dilute stage (typically at a final energy density using the Cooper-Frye prescription [51] to convert the fluid cells into hadron spectra). In AZHYDRO [5, 8] this is done in a longitudinally boost-invariant setup leading to a 2+1 dimensional evolution. In the following we discuss in more detail our modifications to two of the above ingredients, namely the equation of state (Sec. II A) and the initial conditions (Sec. II B).

A. Equation of State

The default AZHYDRO code (version v0.2) [5, 8] employs an equation of state (labeled "EoS-99") consisting of an ideal massless quark-gluon gas at high temperatures and a hadron resonance gas (HRG) in partial chemical equilibrium at low temperatures[1]. The two parts are matched via a Maxwell construction at a critical temperature $T_c = 165$ MeV in a first-order phase transition with a mixed phase, see dashed line in the upper panel of Fig. 1. The sound velocity c_s vanishes in the mixed phase (see the lower panel of Fig. 1), resulting in a vanishing acceleration over a relatively long duration. Consequently, the radial flow of the system largely stalls until the end of the mixed phase. In practice, this implies, e.g., that multistrange particles like the Ω^- baryon have to be decoupled close to the kinetic freezeout of the bulk particles, at $T_{\rm fo} \simeq 100$ MeV, to reproduce the pertinent experimental spectra at RHIC [5].

Recent lattice-QCD (lQCD) calculations have now established that, at vanishing baryon chemical potential ($\mu_B = 0$), the transition between the QGP and hadronic matter is a smooth crossover [25, 26]. The pseudo-critical deconfinement transition temperature obtained by the two leading lQCD groups [26, 52] has now converged to

[1] Recently, a patch was released for AZHYDRO by Molnar and Huovinen wich also contains a lattice-based EoS [45].

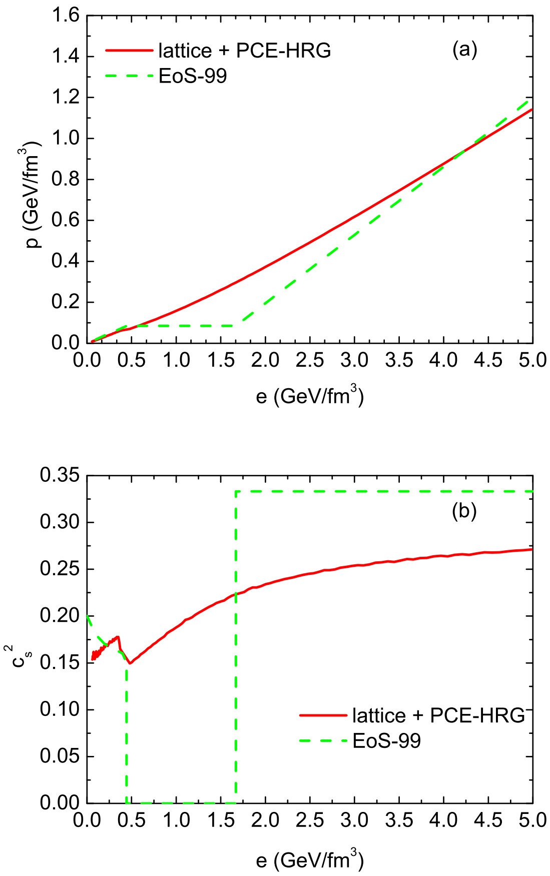

FIG. 1: (Color online) Comparison of pressure (upper panel) and speed of sound squared (lower panel) vs. energy density as obtained from EoS-99 (dashed lines) and our new equation of state (solid lines).

a common value of around $T_c \simeq 170$ MeV [53]. Some differences remain regarding the interaction measure, $I = e - 3p$ [54, 55]. The calculations by the Wuppertal-Budapest (WB) collaboration [55] reproduce the HRG results in chemical equilibrium below T_c, while their lattice action is not ideally suited to the high-T limit where their thermodynamic quantities come out slightly below the results of the HotQCD collaboration [54]. In our fit we decided to employ the WB results in the transition region and to smoothly match on to the HotQCD results for $T \gtrsim 180$ MeV. Once $I(T)$ is specified we calculate the EoS, $p(e)$, following the procedure described in Ref. [55]. The resulting EoS describes strongly interacting matter in thermal and chemical equilibrium. However, in URHICs it is well-known that hadron ratios freeze out at a temperature of $T_{\rm ch} \simeq 160\,$MeV [38–40]. To account for the departure from chemical equilibrium in the hadronic phase below this temperature, we follow the approach in Ref. [56], by introducing effective chemical potentials for hadrons which are stable under strong interactions, i.e., pions, kaons, etas, nucleons and antinucleons, including their feeddown contributions (e.g., $\rho \to 2\pi$ with $\mu_\rho = 2\mu_\pi$), usually referred to as "partial chemical equilibrium (PCE). The conservation of antibaryon number is of particular importance since, in turn, it triggers the build-up of pion chemical potentials [56]. We have verified that the pertinent chemical-equilibrium EoS is consistent with the lQCD results. In the construction of our URHIC EoS we then replace the chemical-equilibrium part with the PCE part. We will refer to the resulting EoS as "latPHG" EoS[2], which is compared to EoS-99 in Fig. 1. As expected, the most notable differences are in the transition regime, where the pressure in the latPHG EoS is enhanced; but, most importantly, the speed of sound remains large, $c_s^2 = \partial p/\partial e \simeq 0.15 - 0.20$, compared to zero in EoS-99. As is well known, this will have significant ramifications for the radial flow, especially toward the end of the transition, $e \simeq 0.5$ GeV/fm^3, and in connection with the kinetic freezeout of multistrange particles.

B. Initial Conditions

Initial conditions currently constitute one of the largest uncertainties in hydrodynamic simulations of URHICs [19]. In default AZHYDRO, a combination of wounded-nucleon and binary-collision density is used to initialize the entropy density,

$$s(\tau_0, x, y; b) = \text{const}\,[0.25\frac{n_{\rm BC}(x,y;b)}{n_{\rm BC}(0,0;0)} + 0.75\frac{n_{\rm WN}(x,y;b)}{n_{\rm WN}(0,0;0)}]\,, \tag{2}$$

at an initial time of $\tau_0 = 0.6$ fm/c for each impact parameter b. This ansatz leads to good agreement with the observed centrality dependence of charged particle multiplicities [5, 57]. Other initial density profiles, e.g., inspired by the CGC, have also been used [58, 59].

However, to accelerate the build-up of radial flow, which is essential for describing spectra of multistrange particles at $T_{\rm ch}$, a compact initial profile with large initial pressure gradients is favored. Such a profile is furthermore an essential ingredient to a realistic description of HBT radii [27]. As a limiting case, we choose the entropy-density profile to be solely proportional to the binary-collision density

$$s(\tau_0, x, y; b) = C(b)\; n_{\rm BC}(x, y; b)\,. \tag{3}$$

While our fits below favor compact profiles they do not necessarily dictate collision scaling, albeit it turns out to work well. We calculate $n_{\rm BC}$ using an optical Glauber model [5, 57]. Compact profiles have also been used in some other hydrodynamic simulations [21, 43, 60]. Since

[2] Following the systematic analysis of hadron observables in Ref. [38] we also introduce a "strangeness suppression" factor $\gamma_s = \gamma_{\bar s} \simeq 0.85$ for each net (anti-) strange quark in a hadron.

the particle multiplicity does not scale with $n_{\rm BC}$, the coefficient in Eq. (3) needs to become b-dependent [43].

Another uncertainty in the initial conditions concerns the possibility of pre-equilibrium flow. In most hydrodynamic simulations, the initial transverse collective velocity is assumed to be zero. However, it has been argued that flow can easily emerge before kinetic equilibrium is established [28, 29]. An initial radial flow field has been implemented into a few calculations and shown to improve the agreement with bulk-hadron data [8, 32] (e.g., by reducing the final v_2 in calculations with PCE in the hadronic EoS, or by improving on the HBT data). In the present work, we go one step further and adopt a non-trivial pre-equilibrium flow field including finite ellipticity. Specifically, we employ the empirical ansatz proposed in Ref. [61], which was successfully used to fit bulk and multistrange observables in a sequential kinetic freezeout scenario [62]. The transverse velocity is parameterized in terms of the spatial coordinates r and ϕ_s as

$$v(r,\phi_s) = \widetilde{r}[\alpha_0 + \alpha_2 \cos(2\phi_b)] \ , \qquad (4)$$

where α_0 quantifies the surface radial flow and α_2 the anisotropy. The azimuthal angle ϕ_b of the flow vector can be tilted away from ϕ_s through

$$\tan\phi_b = \kappa \frac{R_{\rm x}^2}{R_{\rm y}^2} \tan\phi_s \, , \qquad (5)$$

where κ is a tunable parameter dependent on the impact parameter b, and $R_{\rm x} = R_0 - b/2$, $R_{\rm y} = \sqrt{R_0^2 - (b/2)^2}$ are the short and long half-axis of the initial ellipse, and R_0 is the radius of the colliding nuclei (with identical A). Finally, the normalized radius $\widetilde{r}$ in Eq. (4) is

$$\widetilde{r} = \sqrt{\frac{r^2}{R_{\rm x}^2}\cos^2\phi_s + \frac{r^2}{R_{\rm y}^2}\sin^2\phi_s} \ . \qquad (6)$$

We keep the initial time $\tau_0 = 0.6\,{\rm fm}/c$ as in the default AZHYDRO.

III. BULK EVOLUTION

Before turning to quantitative fits to hadron spectra in the following section, we first illustrate the effects of our amendments on the bulk-matter evolution of a fireball in semicentral Au-Au at RHIC. The bulk evolution in a hydrodynamic system can be characterized by the time evolution of the average transverse radial flow, $\langle v_T \rangle$, and of the anisotropy of the energy-momentum tensor [5],

$$\varepsilon_P = \frac{\int dxdy (T^{\rm xx} - T^{\rm yy})}{\int dxdy (T^{\rm xx} + T^{\rm yy})} \ . \qquad (7)$$

In Fig. 2, we compare the longitudinal proper-time evolution of both quantities in default AZHYDRO to simulations with updated EoS and with both updated EoS and modified initial conditions. The parameters for the latter correspond to the final data fit discussed in Sec. IV B.

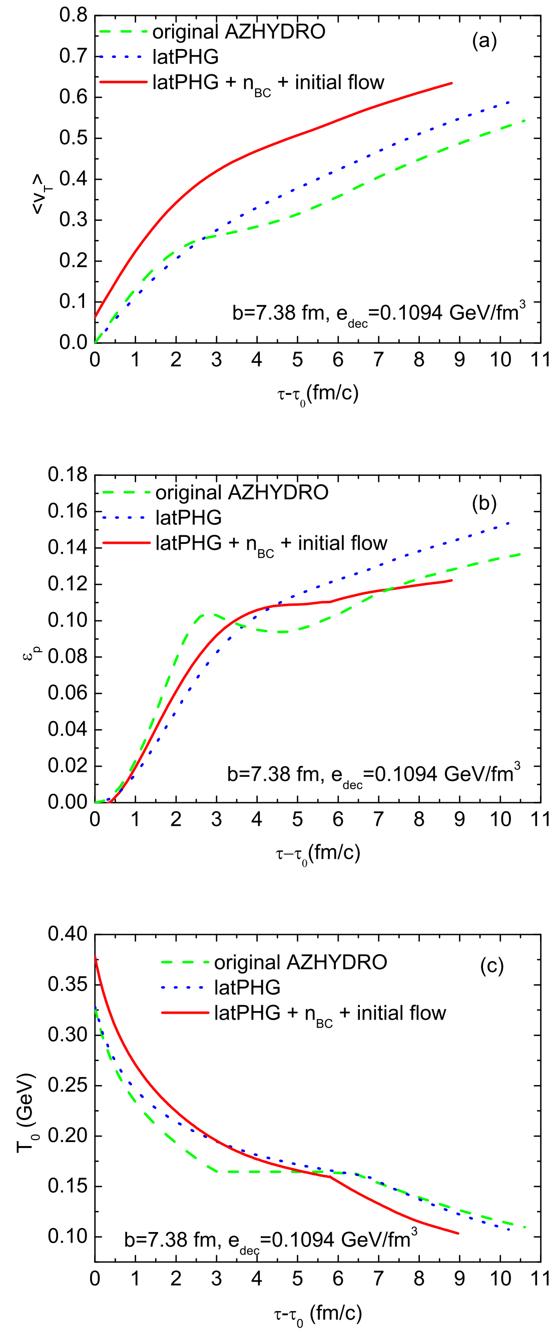

FIG. 2: (Color online) (a) Proper-time evolution of the average transverse radial velocity, $\langle v_T \rangle$, for different hydro scenarios: (i) default AZHYDRO with EoS-99 (green dashed curve), (ii) default AZHYDRO with the new EOS (blue dotted curve), and (iii) the new EoS with initial flow and compact initial density profile (red solid curve). (b) The same comparison for the time evolution of the energy-momentum anisotropy, ε_P. (c) The evolution of the temperature in the central cell of the transverse plane.

Since the new EoS does not feature a vanishing acceleration at (or around) T_c, the knee in $\langle v_T(\tau)\rangle$ and the dip in $\varepsilon_P(\tau)$ disappear. However, the acceleration during the first 3 fm/c is slightly lagging behind in latPHG relative to EoS99 due to the non-ideal behavior of the former. As a result, the total radial flow is not very different at the beginning of the hadronic phase, which also implies that the anisotropy keeps increasing significantly in the hadronic evolution of both scenarios. These (possibly undesired) properties can be modified by introducing more compact initial profiles and initial flow, as shown by the pertinent solid lines in Fig. 2: the radial flow increases by ca. 50% at T_c, while the eccentricity essentially levels off thereafter. Both features are crucial in fitting multistrange particle spectra at T_c, and also improve the description of bulk particles at $T_{\rm fo}$ (in particular the reduced anisotropy, but the increased final flow also helps to describe the p_T spectra out to higher p_T than before). The more rapid expansion of the fireball shortens the lifetime of the fireball by almost 15%, from ~10.6 fm/c in default AZHYDRO to ~9.0 fm/c in the fully amended case (both with $e_{\rm dec} = 0.1094$ GeV/fm^3).

The lower panel in Fig. 2 shows the time evolution of the temperature in the central cell of the transverse plane. While the initial temperature in the fully amended case is higher than in the default AZHYDRO (due to more compact initial-entropy profile), it turns out that the duration of the hadronic phase in the two cases is comparable (note that $T_c = 170$ MeV vs 165 MeV in the amended and default AZHYDRO, respectively).

IV. HADRON OBSERVABLES

The amended AZHYDRO as described above has been utilized to conduct "eye-ball" fits to simultaneously describe spectra and v_2 of bulk and multistrange hadron (at $T_{\rm fo}$ and $T_{\rm ch}$, respectively) in Au-Au collisions at full RHIC energy. We have focused on two centralities, 0-5% ("central") and 20-30% ("semicentral"), which, for simplicity, we have approximated by fixed impact parameters (b=2.3 and 7.38 fm, respectively) corresponding to participant numbers, $N_{\rm part}$, calculated in the optical Glauber model [38] for the two experimental selections. The central initial-entropy density, $s_0 \equiv s(\tau_0, 0, 0; b)$, is then adjusted to the experimental hadron multiplicities for the two centralities, evaluated at kinetic freezeout in the evolution ($e_{\rm fo} = 0.1094$ GeV/fm^3, or $T_{\rm fo} = 110$ MeV) incorporating resonance decays (the spectra and feed-down from multistrange hadrons, for which we assume early kinetic freezeout, are evaluated at $T_{\rm ch} = 160$ MeV). The two parameters in the initial-flow field basically control the radial flow (α_0) and, subsequently, the elliptic flow (α_2). Within our accuracy they turn out centrality-independent, provided the parameter for the "tilt" between position vector and flow vector is suitably increased for more peripheral collisions (which is consistent with intuition, e.g., going to one in the academic limit of b=0). The resulting parameter values are summarized in Tab. I. The kinetic freezeout temperature, $T_{\rm fo} = 110$ MeV, also turns out to be identical for the two centrality classes within our accuracy.

	s_0 (fm^{-3})	T_0 (MeV)	α_0	α_2	κ
0-5%	159.5	399.9	0.13	0.004	1.0
20-30%	133.1	377.9	0.13	0.004	4.2

TABLE I: Initialization parameters for central (0-5%, b = 2.3 fm) and semicentral (20-30%, b = 7.38 fm) Au-Au ($\sqrt{s_{NN}}$=200 GeV) collisions; s_0 is the initial-entropy density in the center of the transverse plane and T_0 is the pertinent temperature resulting from a collision-density overlap; α_0, α_2 and κ parameterize the initial anisotropic flow profile, cf. Sec. II B.

A few remarks are in order concerning the applicability of hydrodynamics in the (later stages of the) hadronic phase. It is often argued that the latter carries large viscosity thus mandating a transport treatment. However, there are several arguments suggesting that the hadronic evolution in URHICs does not carry large η/s ratios. First, since the QCD transition at μ_B=0 is presumably close to a second order one, it is likely that η/s possesses a minimum around the pseudocritical temperature of $T_c \simeq 170$ MeV. The question then is how fast η/s increases with decreasing T [63–66]. Dilepton measurements (and pertinent calculations) at the SPS show that the average ρ-meson width in the hadronic phase is substantially broadened, by more than 200 MeV (cf. Ref. [67] for a recent review). This corresponds to a mean-free-path of below 1 fm, and is comparable to the thermal kinetic energy of the ρ, $KE \simeq 1.5T \simeq 225$ MeV. Even at thermal freezeout the ρ is still broadened by ca. 100 MeV. From another angle, but using similar techniques (*i.e.*, effective hadronic interactions), charm diffusion has been evaluated in hadronic matter in Ref. [68]. While the diffusion coefficient (which, in units of the thermal wavelength, $1/(2\pi T)$, is roughly proportional to η/s) increases appreciably toward lower temperatures in equilibrium matter, the inclusion of effective chemical potentials only leads to a ~30% increase when going down from T=170 MeV to 100 MeV. We thus believe that viscosity effects in hadronic matter as formed in URHICs may be significantly smaller than commonly assumed.

In the following sections we present the results for the observables, starting with inclusive yields (hadrochemistry, Sec. IV A) and then becoming more differential with p_t spectra (Sec. IV B) and azimuthal dependencies (Sec. IV C).

A. Particle Yields

The PCE part of our EoS ensures that the stable-hadron numbers are approximately conserved between chemical and thermal freezeout. In Tab. II we compare our π, K and p multiplicities in central Au-Au collisions, calculated at $T_{\rm fo}$, to STAR [38] and PHENIX [69] data. Since we employ the chemical freezeout temperature we adjusted the total entropy to obtain the central value of the proton number measured by STAR (including weak feeddown); consequently, the calculated π (corrected for weak feeddown), K and $\bar{p}$ yields are within the experimental errors (residual deviations inside the errors may be caused, e.g., by slight variations in the hadronic resonances included in the EoS). Good agreement is also found with the kaon measurements of PHENIX, while the calculated pion yields are slightly above the 1-σ upper limit of the PHENIX pions (which include weak feeddown). A more significant discrepancy arises with the PHENIX anti-/protons (weak feeddown corrected). Similar findings are reported in other hydro-model fits [43, 70]. We note that a slightly higher centrality selection in the PHENIX data could still be compatible with our calculated kaons while improving the agreement with pions and anti-/protons.

B. Single-Particle Spectra

Let us first turn to the multistrange hadron spectra (ϕ, Ξ and Ω) which we evaluate at the chemical-freezeout temperature, $T_{\rm ch}$ = 160 MeV, where the energy density is $e_{\rm ch}$ = 0.372 GeV/fm^3. As an additional centrality class we consider $20-40\%$ central Au-Au collision which we approximate with b = 8.04 fm with an initial-entropy density in the center of the transverse plane of $s_0 = 130.9$ fm^{-3} to reproduce the pertinent bulk-particle yields; all other parameters are the same as for $20-30\%$ centrality (including the strangeness suppression factor of γ_s = 0.85 [38]). The comparison of our calculated multistrange hadron spectra to STAR measurements are shown in Fig. 3, showing good agreement in both central and semicentral collisions. As typical for hydrodynamic simulations, the description extends to slightly higher p_T for higher centrality, here up to $p_T \simeq 4-5$ GeV for hyperons.

With the same set of parameters, the freezeout of bulk particles, (π, K, p) is evaluated at $T_{\rm fo}$ = 110 MeV (at an energy density of $e_{\rm fo}$ = 0.1094 GeV/fm^3). This is consistent with values extracted from systematic blast-wave fits performed by the experimental collaborations to their data [38, 74]. Consequently, our calculated spectra agree well with their spectra as well, cf. Fig. 4 albeit with absolute normalization owing to the implementation of chemical freezeout. One exception are the PHENIX protons (including weak feeddown corrections from hyperons): while the spectral shape is well described, a renormalization factor of 0.71 needs to be applied for an optimal description of the absolute yields (in accord with discussion in Sec. IV A and Tab. II).

In Ref. [43], which employs an EoS similar to that used in AZHYDRO, it was deduced that bulk-particle spectra can be fitted better with a chemical freezeout temperature of 150 MeV, ca. 10 MeV lower than the value suggested by statistical model fits [38–40]. Our results indicate that with a modern lattice EoS and initial flow the chemical freezeout temperature in hydrodynamics can be made compatible with statistical model fits.

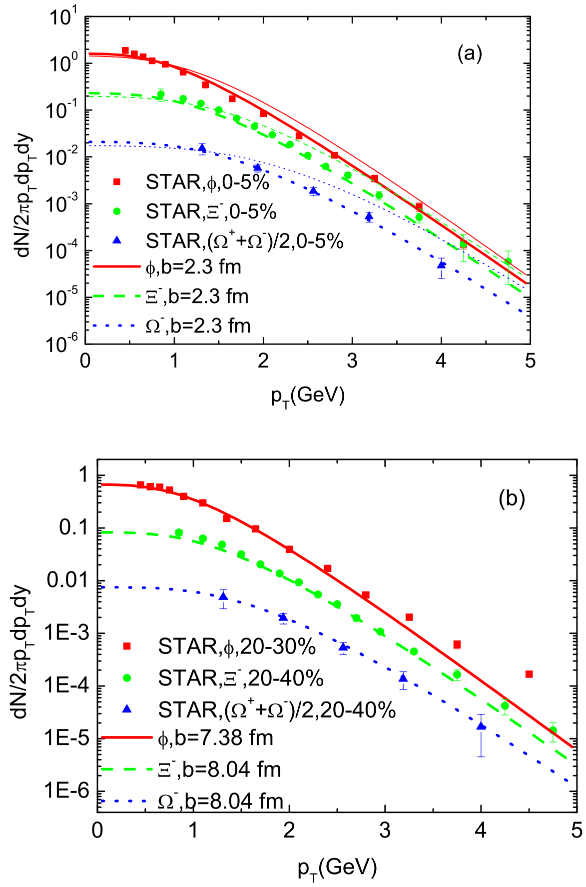

FIG. 3: (Color online) (a) Our calculated p_T-spectra of multistrange particles (ϕ, Ξ and Ω) in 0-5% central Au-Au collisions compared to STAR data [71, 72]; the thick (thin) lines correspond to kinetic freezeout at $T_{\rm ch} = 160$ MeV ($T_{\rm fo} = 110$ MeV, with identical normalization). (b) The same comparison for semicentral collisions (without thin lines for late freezeout).

To illustrate the significance of the early freezeout of multistrange hadrons in our calculations, we also plot their spectra at $T_{\rm fo} = 110$ MeV in central Au-Au (thin lines in the upper panel of Fig. 3). One sees that the additional radial flow developed in the hadronic phase hardens the spectra substantially leading to a systematic overprediction of the data with increasing p_T. The discrepancy is largest for the Ω^- and less pronounced for the Ξ and ϕ. The latter may not be surprising; e.g., the Ξ possesses one light valence quark and at least one pion-resonance excitation ($\Xi(1530)$), while the ϕ couples strongly to both $\pi\rho$ and $K\bar{K}$ channels. Thus both ϕ and Ξ might develop a reaction rate in hadronic matter which

$\mathrm{d}N/\mathrm{d}y$	π^+	π^-	K^+	K^-	p	$\bar{p}$
STAR	322 ± 25	327 ± 25	51.3 ± 6.5	49.5 ± 6.2	34.7 ± 4.4	26.7 ± 3.4
PHENIX	286.4 ± 24.2	281.8 ± 22.8	48.9 ± 5.2	45.7 ± 5.2	18.4 ± 2.6	13.5 ± 1.8
Y feeddown included	312.2	314.4	48.2	48.4	34.0	26.2
Y feeddown subtracted	303.1	303.1	48.1	48.2	25.8	19.9

TABLE II: Comparison of the calculated bulk-particle yields with STAR and PHENIX measurements at midrapidity in 0-5% central Au-Au collisions at $\sqrt{s_{\rm NN}} = 200$ GeV. Results are shown with and without feeddown from hyperon decays. The initial entropy has been adjusted to reproduce the observed STAR anti-/protons [38]. The STAR pions are weak feeddown corrected, while the protons and anti-protons include hyperon feeddown. PHENIX anti-/protons are weak feeddown corrected [69], but not the pions.

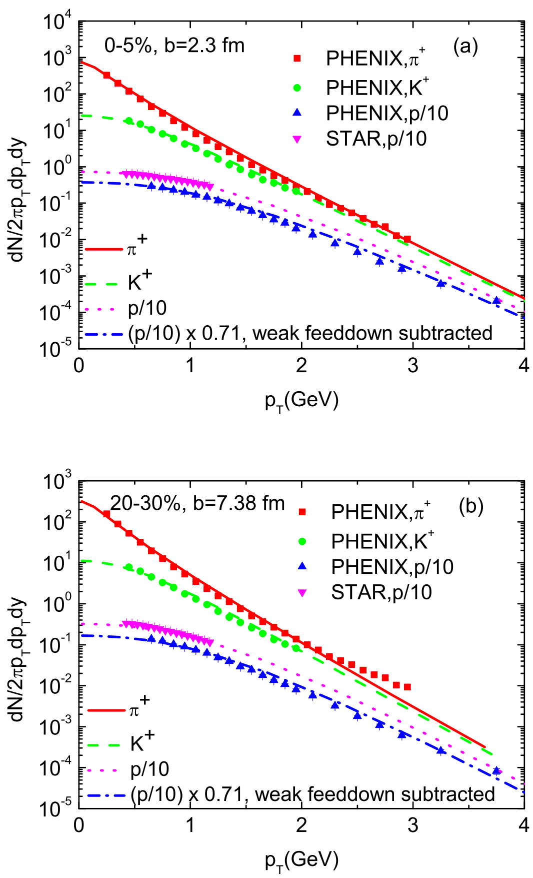

FIG. 4: (Color online) (a) Our calculated p_T spectra of bulk particles (π^+, K^+ and p) in 0-5% central Au-Au collisions compared to PHENIX [69] and STAR data [73]. (b) The same comparison for semicentral collisions.

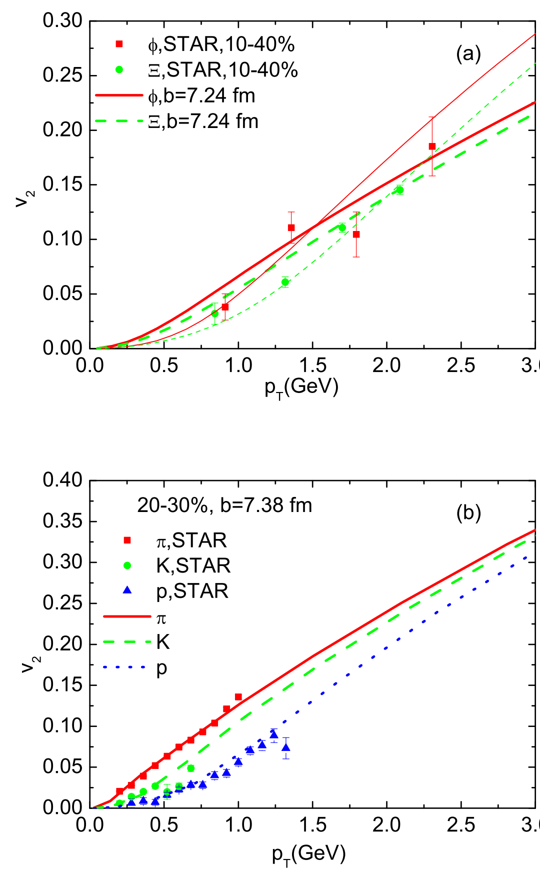

FIG. 5: (Color online) (a) Our calculations for the elliptic-flow coefficient as a function of p_T for ϕ and Ξ compared to STAR data [72, 76] in 10-40% central Au-Au collisions; the thick (thin) lines correspond to kinetic freezeout at $T_{\rm ch} = 160\,\mathrm{MeV}$ ($T_{\rm fo} = 110\,\mathrm{MeV}$, with identical normalization); the calculations employ the same impact parameter as for the 20-30% centrality class. (b) The same comparison for π, K and p with STAR data for 20-30% centrality from Ref. [77]; only the results for $T_{\rm fo} = 110\,\mathrm{MeV}$ are shown.

allows them to pick up some additional collectivity after chemical freezeout, leading to an effective freezeout temperature slightly below $T_{\rm ch}$; similar findings are reported in Ref. [33] for the ϕ.

C. Elliptic Flow

We finally turn to the elliptic flow, which in our calculation is controlled, to a limited extent, by the parameters α_2 and κ characterizing the anisotropy of initial flow, and, to a lesser extent, by the interplay with the initial radial flow (the initial spatial anisotropy is fixed by our assumption of the $n_{\rm BC}$ profile of the entropy density). As is well known [5, 6, 9, 75], the v_2 of massive particles is reduced at low p_T by a large radial flow. This, in particular, also occurs when initial flow fields are introduced [8], thus mitigating the problem of a growing pion v_2 in the hadronic phase when a PCE EoS is employed [8, 43, 44].

Our results for the anisotropy coefficient of multistrange and bulk particles in semicentral Au-Au collisions are compared to STAR data in the upper and lower panel of Fig. 5, respectively. Our fit yields fairly good agreement for both hadron classes. Clearly, the aforementioned problem of previous PCE implementations is largely resolved due to our more explosive expansion, in connection with initial flow fields, which suppress a significant increase of v_2 in the late stage of the hydrodynamic evolution. This was already indicated by the saturation of the anisotropy of the energy-momentum tensor anisotropy in Fig. 2.

To illustrate the significance of sequential freezeout, we display again the v_2 of ϕ and Ξ at $T_{\rm fo} = 110\,\mathrm{MeV}$ by thin lines in the upper panel of Fig. 5. Compared to the p_T spectra (the upper panel of Fig. 3), the current v_2 data are less discriminatory for the freezeout temperature of multistrange hadrons. In accordance with the remarks at the end of Sec. IV B, the v_2 of Ξ may also favor a kinetic-freezeout temperature slightly below $T_{\rm ch}$.

V. SUMMARY AND CONCLUSION

In the present study we have explored the capability of ideal hydrodynamics to simultaneously and quantitatively describe bulk- and multistrange-hadron spectra and v_2 in Au-Au collisions at RHIC. Specifically, we have augmented an existing 2+1D ideal hydro code by (i) an equation of state compatible with recent lattice QCD data matched to a hadron resonance gas in partial chemical equilibrium, (ii) a sequential kinetic freezeout of multistrange and bulk particles, and (iii) a compact initial density profile with non-zero radial and elliptic flow. We deem these amendments "reasonable" in the sense of being either suggested by theory (lattice EoS), experiment (chemical freezeout) and empirical fits (early kinetic freezeout of multistrange hadrons), or at least plausible (initial flow and compact profiles). The above items also encompass three of the four components identified for solving the pion HBT problem. The main practical consequences of the modifications are a more rapid build-up of the radial and elliptic flow, where the latter essentially levels off after hadronization. Phenomenologically, the underlying parameters (basically the three in the initial-flow field parametrization) can be adjusted as to render multistrange hadrons' kinetic freezeout at $T_{\rm ch}$ compatible with data, and to subsequently avoid an overshooting of the bulk-particle v_2 at $T_{\rm fo}$. We consider this a significant improvement over existing ideal-hydro calculations, thereby corroborating the empirical picture of early freezeout of multistrange hadrons.

We did not include the effects of viscosities nor of initial-state fluctuations, which are both clearly needed for realistic hydrodynamic simulations of heavy-ion collisions. However, we believe that our study can still serve as a useful baseline for the effects we have included. In addition, we anticipate that our amended AZHYDRO can be a valuable tool as a realistic fireball background for evaluating heavy-quark(onium) and electromagnetic probes.

Acknowledgments

MH acknowledges useful correspondence with C. Shen and E. Frodermann. We thank U. Heinz and C. Shen for valuable comments on the manuscript. This work was supported by the U.S. National Science Foundation (NSF) through CAREER grant PHY-0847538 and grant PHY-0969394, by the A.-v.-Humboldt Foundation, by the RIKEN/BNL Research Center and DOE grant DE-AC02-98CH10886, and by the JET Collaboration and DOE grant DE-FG02-10ER41682.

[1] J. Adams *et al.* [STAR Collaboration], Nucl. Phys. **A757**, 102 (2005); K. Adcox *et al.* [PHENIX Collaboration], Nucl. Phys. **A757**, 184 (2005); I. Arsene *et al.* [BRAHMS Collaboration], Nucl. Phys. **A757**, 1 (2005); B. B. Back *et al.* [PHOBOS Collaboration] , Nucl. Phys. **A757**, 28 (2005).

[2] K. Aamodt *et al.* [ALICE Collaboration], Phys. Rev. Lett. **105**, 252302 (2010); G. Aad *et al.* [ATLAS Collaboration], Phys. Rev. Lett. **105**, 252303 (2010).

[3] M. Gyulassy and L. McLerran, Nucl. Phys. **A750**, 30 (2005).

[4] E. Shuryak, Prog. Part. Nucl. Phys. **62**, 48 (2009).

[5] P.F. Kolb and U.W. Heinz, In R. C. Hwa (ed.) et al.: Quark gluon plasma, 634, [nucl-th/0305084]; P.F. Kolb, J. Sollfrank, and U.W. Heinz, Phys. Rev. **C62**, 054909 (2000).

[6] D. Teaney, J. Lauret, and E.V. Shuryak, *preprint* nucl-th/0110037.

[7] T. Hirano and K. Tsuda, Phys. Rev. **C66**, 054905 (2002).

[8] P. F. Kolb and R. Rapp, Phys. Rev. **C67**, 044903 (2003).

[9] P. Huovinen and P.V. Ruuskanen, Ann. Rev. Nucl. Part. Sci. **56**, 163 (2006).

[10] C. Nonaka and S. A. Bass, Phys. Rev. **C75**, 014902 (2007).
[11] Y. Hama *et al.*, Nucl. Phys. **A774**, 169-178 (2006).
[12] H. Niemi, K. J. Eskola, and P. V. Ruuskanen, Phys. Rev. **C79**, 024903 (2009).
[13] B. Schenke, S. Jeon, and C. Gale, Phys. Rev. **C82**, 014903 (2010).
[14] R. J. Fries and C. Nonaka, Prog. Part. Nucl. Phys. **66**, 607 (2011).
[15] P. Romatschke and U. Romatschke, Phys. Rev. Lett. **99**, 172301 (2007).
[16] H. Song and U. W. Heinz, Phys. Rev. **C77**, 064901 (2008).
[17] K. Dusling and D. Teaney, Phys. Rev. **C77**, 034905 (2008).
[18] U. Heinz, in R. S. Stock (ed.), *Relativistic Heavy Ion Physics*, Landolt-Boernstein New Series, I/23, Springer Verlag, New York (2010).
[19] H. Song, S. A. Bass, U. Heinz, T. Hirano, and C. Shen, Phys. Rev. Lett. **106**, 192301 (2011); Phys. Rev. **C83**, 054910 (2011).
[20] B. Schenke, S. Jeon, and C. Gale, Phys. Rev. Lett. **106**, 042301 (2011).
[21] H. Niemi, G. S. Denicol, P. Huovinen, E. Molnar, and D. H. Rischke, Phys. Rev. Lett. **106**, 212302 (2011).
[22] V. Roy and A. K. Chaudhuri, Phys. Lett. **B703**, 313 (2011).
[23] C. Shen, U. Heinz, P. Huovinen, and H. Song, Phys. Rev. **C84**, 044903 (2011).
[24] P. Huovinen, Nucl. Phys. **A761**, 296 (2005).
[25] Y. Aoki, G. Endrodi, Z. Fodor, S. D. Katz, and K. K. Szabo, Nature **443**, 675 (2006).
[26] M. Cheng *et al.*, Phys. Rev. **D81**, 054504 (2010).
[27] S. Pratt, Phys. Rev. Lett. **102**, 232301 (2009); S. Pratt and J. Vredevoogd, Phys. Rev. **C78**, 054906 (2008).
[28] J. Vredevoogd and S. Pratt, Phys. Rev. **C79**, 044915 (2009).
[29] R. J. Fries, J. I. Kapusta, and Y. Li, Nucl. Phys. **A774**, 861 (2006).
[30] U. W. Heinz and S. M. H. Wong, Phys. Rev. **C66**, 014907 (2002).
[31] A. Krasnitz, Y. Nara, and R. Venugopalan, Phys. Lett. **B554**, 21 (2003).
[32] W. Broniowski, W. Florkowski, M. Chojnacki, and A. Kisiel, Phys. Rev. **C80**, 034902 (2009).
[33] T. Hirano, U. W. Heinz, D. Kharzeev, R. Lacey, and Y. Nara, Phys. Lett. **B636**, 299 (2006); Phys. Rev. **C77**, 044909 (2008).
[34] Z. Qiu, C. Shen, and U. W. Heinz, *preprint* arXiv:1110.3033 [nucl-th].
[35] S. A. Bass and A. Dumitru, Phys. Rev. **C61**, 064909 (2000).
[36] R. Rapp and E. V. Shuryak, Phys. Rev. Lett. **86**, 2980 (2001).
[37] C. Greiner and S. Leupold, J. Phys. **G27**, L95 (2001).
[38] B. I. Abelev *et al.* [STAR Collaboration], Phys. Rev. **C79**, 034909 (2009).
[39] P. Braun-Munzinger, K. Redlich, and J. Stachel, In R. C. Hwa (ed.) et al.: Quark gluon plasma, 491, [nucl-th/0304013].
[40] F. Becattini, J. Cleymans, A. Keranen, E. Suhonen, and K. Redlich, Phys. Rev. **C64**, 024901 (2001).
[41] H. Bebie, P. Gerber, J. L. Goity, and H. Leutwyler, Nucl. Phys. **B378**, 95 (1992).
[42] D. Teaney, *preprint* nucl-th/0204023.
[43] P. Huovinen, Eur. Phys. J. **A37**, 121 (2008).
[44] T. Hirano and M. Gyulassy, Nucl. Phys. **A769**, 71 (2006).
[45] P. Huovinen and P. Petreczky, Nucl. Phys. **A837**, 26 (2010).
[46] C. Shen, U. Heinz, P. Huovinen, and H. Song, Phys. Rev. **C82**, 054904 (2010).
[47] A. Shor, Phys. Rev. Lett. **54**, 1122 (1985).
[48] H. van Hecke, H. Sorge, and N. Xu, Phys. Rev. Lett. **81**, 5764 (1998).
[49] N. Xu, Nucl. Phys. **A787**, 44 (2007).
[50] B.I. Abelev *et al.* [STAR Collaboration], Phys. Rev. **C79**, 064903 (2009).
[51] F. Cooper and G. Frye, Phys. Rev. **D10**, 186 (1974).
[52] S. Borsanyi *et al.* [Wuppertal-Budapest Collaboration], JHEP **1009**, 073 (2010).
[53] Y. Aoki *et al.*, JHEP **0906**, 088 (2009).
[54] W. Soldner [HotQCD Collaboration], PoS **LATTICE2010**, 215 (2010).
[55] S. Borsanyi *et al.*, JHEP **1011**, 077 (2010).
[56] R. Rapp, Phys. Rev. **C66**, 017901 (2002).
[57] P. F. Kolb, U. W. Heinz, P. Huovinen, K. J. Eskola, and K. Tuominen, Nucl. Phys. **A696**, 197-215 (2001).
[58] D. Kharzeev, E. Levin, and M. Nardi, Nucl. Phys. **A730**, 448-459 (2004).
[59] H.-J. Drescher and Y. Nara, Phys. Rev. **C75**, 034905 (2007).
[60] W. Broniowski, M. Chojnacki, W. Florkowski, and A. Kisiel, Phys. Rev. Lett. **101**, 022301 (2008).
[61] F. Retiere and M. A. Lisa, Phys. Rev. **C70**, 044907 (2004).
[62] M. He, R. J. Fries, and R. Rapp, Phys. Rev. **C82**, 034907 (2010).
[63] M. Prakash, M. Prakash, R. Venugopalan, and G. Welke, Phys. Rept. **227**, 321 (1993).
[64] L. P. Csernai, J. .I. Kapusta, and L. D. McLerran, Phys. Rev. Lett. **97**, 152303 (2006).
[65] J. W. Chen, Y. H. Li, Y. F. Liu, and E. Nakano, Phys. Rev. **D76**, 114011 (2007).
[66] P. Chakraborty and J. I. Kapusta, Phys. Rev. **C83**, 014906 (2011).
[67] R. Rapp, J. Wambach, and H. van Hees, arXiv:0901.3289 [hep-ph].
[68] M. He, R. J. Fries, and R. Rapp, Phys. Lett. **B701**, 445 (2011).
[69] S. S. Adler *et al.* [PHENIX Collaboration], Phys. Rev. **C69**, 034909 (2004).
[70] P. Huovinen, priv. comm. (2011).
[71] J. Adams *et al.* [STAR Collaboration], Phys. Rev. Lett. **98**, 062301 (2007).
[72] B. I. Abelev *et al.* [STAR Collaboration], Phys. Rev. Lett. **99**, 112301 (2007).
[73] J. Adams *et al.* [STAR Collaboration], Phys. Rev. Lett. **92**, 112301 (2004).
[74] J.M. Burward-Hoy [PHENIX Collaboration], Nucl. Phys. **A715**, 498 (2003).
[75] P. Huovinen, P. F. Kolb, U. W. Heinz, P. V. Ruuskanen, and S. A. Voloshin, Phys. Lett. **B503**, 58 (2001).
[76] B. I. Abelev *et al.* [STAR Collaboration], Phys. Rev. **C77**, 054901 (2008).
[77] J. Adams *et al.* [STAR Collaboration], Phys. Rev. **C72**, 014904 (2005).